*Journal of Reproduction and Development, Vol. 63, No 3, 2017*

**—Original Article—**

# Investigating right ovary degeneration in chick embryos by transcriptome sequencing

**Jianning YU[1)], Leyan YAN[1)], Zhe CHEN[1)], Hui LI[1)], Shijia YING[1)], Huanxi ZHU[1)] and Zhendan SHI[1)]**

[1)]*Laboratory of Animal Breeding and Reproduction, Institute of Animal Science, Jiangsu Academy of Agricultural Sciences, Nanjing 210014, China*

**Abstract.** In asymmetric chick gonads, the left and right female gonads undergo distinct programs during development, generating a functional ovary on the left side only. Despite some progress being made in recent years, the mechanisms of molecular regulation remain incompletely understood, and little genomic information is available regarding the degeneration of the right ovary in the chick embryo testis. In this study, we performed transcriptome sequencing to investigate differentially expressed genes in the left and right ovaries and gene functions at two critical time points; embryonic days 6 (E6) and 10 (E10). Using high-throughput RNA-sequencing technologies, 539 and 1046 genes were identified as being significantly differentially expressed between 6R-VS-6L and 10R-VS-10L. Gene ontology analysis of the differentially expressed genes revealed enrichment in functional pathways. Among these, candidate genes associated with degeneration of the right ovary in the chick embryo were identified. Identification of a pathway involved in ovarian degeneration provides an important resource for the further study of its molecular mechanisms and functions.

**Key words:** Chick embryo, Degeneration, Right ovary, Transcriptome sequencing

(**J. Reprod. Dev. 63:** 295–303, 2017)

Ovary development and oogonia formation require the serial regulation of specific genes and signaling pathways. In contrast to the testis [1, 2], ovary differentiation is not well characterized. In chicken, in which the male is the homogametic sex (ZZ) and the female is the heterogametic sex (ZW), gonadal morphological differentiation begins between day 5.5 and 6.5. In female embryos, only the left gonad develops into an ovary, while the right gonad regresses. In male embryos, bilateral testis differentiation occurs [3]. However, what regulates meiosis and how ovarian germ cells adopt their specific fate during the embryonic stage are still unclear. Identification of novel regulators of embryonic ovarian and testis differentiation is therefore required and will greatly improve our understanding of normal and aberrant gonad sexual differentiation [4].

High-throughput paired-end RNA sequencing (RNA-seq) has been used to evaluate gene expression at the onset gonadal sex differentiation in embryonic chicken gonads. In recent years, next generation sequencing techniques, such as Solexa/Illumina (Illumina), 454 (Roche), and SOLID (ABI) platforms have emerged as useful tools for transcriptome analyses. These tools have been widely used to investigate gene expression, identify novel transcripts, and to identify differentially expressed genes [5–9]. De novo transcriptome assembly from RNA-seq generates a genome-scale transcriptome map that contains the transcriptional structure and the expression level for each gene in model organisms such as Litchi [10], Chinese bayberry [11], Sugarcane [12], and Asian clam [13]. Illumina sequencing generates many more sequences, with higher coverage and at lower costs than other sequencing technologies. Compared with other transcriptome assemblers, the Trinity recovers more full-length transcripts with a broad range of expression levels, with sensitivity similar to methods that rely on genome alignments [5].

Numerous studies have analyzed the molecular cascade activated in the course of right ovary degeneration in the chick embryo. However, the molecular mechanisms responsible remain controversial. Studies have shown that ovary degeneration is a complex physiological process, regulated in different ways, and that cellular apoptosis may be a potential regulatory mechanism. Apoptosis was first described in 1972 and is the process through which individual cells of multicellular organisms undergo systematic self-destruction in response to a wide variety of stimuli [14]. Apoptosis can be activated in various ways, and studies have shown that signals can be modified by two general mechanisms: death receptor-mediated events and mitochondria-mediated events. In addition, the morphological changes that occur during apoptosis are orchestrated by the proteolytic activity of caspase proteases [15–17], which cleave multiple proteins to orchestrate apoptotic processes [18]. One class inhibits apoptosis (BCL-2, BCL-XL, MCL-1, etc.), a second class promotes apoptosis (BAX, BAK), and a third class, termed the *BH3-only proteins* (BAD, BIK, BID, BIM, BOK, etc.), binds and regulates the anti-apoptotic BCL-2 proteins to promote apoptosis [16]. The intrinsic death pathway is induced by different stress signals, including DNA-damaging agents, viral and cellular oncogenes, and transcriptional blockade [19, 20].

Received: September 16, 2016
Accepted: March 3, 2017
Published online in J-STAGE: April 13, 2017

Correspondence: Z Chen (e-mail: chenzzju@163.com)

## Materials and Methods

*Sample preparation and RNA extraction*

The gonadal morphology of early chick embryos was determined (using PCR) prior to further experimentation. The primer sequences, CHD1F—GTTACTGATTCGTCTACGAGA and CHD1R—ATTGAAATGATCCAGTGCTTG, were used. The PCR result in shown in Supplementary Fig. 1 (online only; samples with two bands represent females and samples with one band represent males. Chick embryonic ovary cells obtained from the left and right ovary at 6 and 10 days were maintained and cultured with high glucose (4.5 g D/L-glucose) Dulbecco's Modified Eagle Medium DMEM-HG (Life Technologies, NY, USA) supplemented with 10% (v/v) fetal bovine serum at 37°C, 5% $CO_2$. 6R: Right ovary of the chick embryo at day 6; 6L: left ovary of the chick embryo at day 6; 10R: right ovary of the chick embryo at day 10; 10L: left ovary of the chick embryo at day 10.

Total RNA was extracted using TRIzol reagent (Invitrogen, Carlsbad, CA, USA) following the manufacturer's protocol, and then treated with RNase-free DNase I. All ovarian samples were pooled prior to library preparation for each experimental group. Equimolar quantities of RNA from each ovarian sample were pooled. Samples were mixed with fragmentation buffer (Ambion, Carlsbad, CA, USA), mRNA was fragmented into short 200-base fragments, and the quality and quantity were determined and quantified using a QUBIT RNA ASSAY KIT and 2100 Bioanalyzer (Agilent Technologies, Santa Clara, CA, USA). Total RNA was reverse transcribed using a RevertAid First Strand cDNA Synthesis Kit (Thermo Scientific, Carlsbad, CA, USA). Next, the short cDNA fragments were ligated with Illumina PE adapters and further amplified by PCR to construct the final cDNA library. This procedure ensures the removal of ribosomal RNA and first-strand cDNA before PCR amplification; therefore, reads are consistent with the orientation of the RNA. The cDNA library was sequenced with the Illumina sequencing platform (Illumina HiSeq™ 2000) using single-end paired-end technology in a single run, by Beijing Genomics Institute (BGI)-Shenzhen, Shenzhen, China.

Raw reads were filtered into clean reads, which were then aligned to the reference chick genome Sscrofa10.2 with SOAPaligner/SOAP2. No more than five mismatches were allowed in the alignment. After that, we proceeded with the deep analyses, including gene expression, gene structure refinement, alternative splicing (AS), and single nucleotide polymorphism (SNP) analysis.

*Preprocessing of RNA-seq data*

Reference unigenes were assembled from the transcriptome (SRA accession SRP018044), and further annotated using the non-redundant protein (Nr) database, nucleotide collection (Nt) database, Swiss-Plot, gene ontology database (GO), clusters of orthologous groups (COG), and Kyoto encyclopedia of genes and genomes (KEGG) [21]. All raw reads were removed, and the reads with a high N content (over 3%) and low quality (the full length of a read N50 bp or over 50% of the bases in a read had a quality value of $\leq 3$) were filtered. At the same time, the Q20, Q30, and GC content of the clean data were summarized. All subsequent analyses were based on these clean datasets. The sequence data were directly downloaded from the Genome website (http://www.ncbi.nlm.nih.gov/genome/111?project_id=10808). An index of the reference genome was built using Bowtie v2.0.6, and paired-end clean reads were aligned to the reference genome using Top Hat v2.0.9 [22].

*Analysis of differential expression*

To identify genes showing a significant change in expression at two different time points, differently expressed genes were estimated from the number of reads per kilobase per million mapped reads (RPKM) [23]. According to the method described by Audic and Claverie, we determined the cut-off values to select the differentially expressed genes. In order to quantify expression, the coverage of each transcript was computed by applying BEDtools v. 2.9.0 [24]. The coverage from all libraries was then combined into a single file. This file was analyzed in R v. 3.0.1 with the bioconductor package 'DEGseq' v. 1.2 [25]. Based on this method, it is possible to evaluate probability counts that are more or less frequent between groups. All transcripts that were differentially expressed between the two groups qualified for annotation. The resulting P-values were fit, and the threshold for significantly differential expression was selected as a corrected P value of 0.05 and log2 (fold change).

*GO and KEGG metabolic pathway analysis*

GO is an international standardized functional classification system that provides a dynamic, updated, controlled vocabulary and a strictly defined concept to comprehensively describe the properties of genes and their products in any organism. In the gene expression profiling analysis, differentially expressed genes were determined using the GOseq package, and the enriched GO categories were identified based on the best 20 blastx hits from the Nr database using the Blast2GO program.

Different genes usually cooperate with each other to exercise their biological functions. Pathway-based analysis helps to further understand the biological functions of genes. Pathway enrichment analysis is carried out by the KEGG database and software programs. Within the KEGG databases, the pathway database contains information on networks of molecular interaction with cells, as well as variations specific to particular organisms. To ensure the credibility of the results, a Bonferroni-corrected P-value of 0.05 was considered to be statistically significant.

*Real-time PCR validation*

Total RNA was extracted from independent biological replicates using Qiagen's Plant RNA Extraction Kit, according to the manufacturer's protocol. The reaction was carried out at 37°C for 10 min followed by heat inactivation at 65°C for 10 min. DNase-treated RNA (2.5 μg) was used for cDNA synthesis with reverse transcriptase (BioRad, Hercules, CA, USA) in accordance with the manufacturer's protocol. The expression of actin (ACT7) was found to be stable in the transcriptome database and was used as the internal control for RT-PCR. Primers were designed for selected transcripts from the transcriptome database and real time PCR was performed using SYBR green I master mix (Roche, GmBH, Basel, Switzerland) on the CFX-Connect™ Real time system (BioRad). Relative expression of the transcripts was calculated using the ΔΔCt method.

**Table 1.** Q20-contents of 6R, 6L, 10R, and 10L

| | 6R | 6L | 10R | 10L |
|---|---|---|---|---|
| Raw reads | 31,066,414 | 31,900,200 | 31,400,070 | 35,504,746 |
| Total clean reads | 30,541,030 | 31,293,780 | 30,759,406 | 34,331,076 |
| $Q_{20}$ (%) | 98.70 | 98.71 | 98.60 | 98.77 |
| $Q_{30}$ (%) | 96.90 | 96.93 | 96.68 | 97.06 |
| GC (%) | 51.39 | 51.05 | 49.90 | 50.04 |
| N (%) | 0.00 | 0.00 | 0.00 | 0.00 |

6R: Right ovary of the chick embryo at day 6; 6L: left ovary of the chick embryo at day 6; 10R: right ovary of the chick embryo at day 10; 10L: left ovary of the chick embryo at day 10.

**Table 2.** The distributions of mapped reads from 6R, 6L, 10R, and 10L

| | 6R | 6L | 10R | 10L |
|---|---|---|---|---|
| Total reads | 30,529,752 | 31,279,308 | 30,746,858 | 34,299,670 |
| Unmapped reads | 5,550,404 | 5,671,414 | 5,353,430 | 6,175,002 |
| Unique mapped reads | 24,837,882 | 25,475,666 | 25,278,336 | 27,993,864 |
| Multiple mapped | 141,406 | 132,228 | 115,092 | 130,804 |
| Mapping ratio (%) | 81.82 | 81.87 | 82.59 | 82.00 |

6R: Right ovary of the chick embryo at day 6; 6L: left ovary of the chick embryo at day 6; 10R: right ovary of the chick embryo at day 10; 10L: left ovary of the chick embryo at day 10.

## Results

### *Illumina sequencing and de novo assembly*

RNA-seq is a useful approach for obtaining a complete set of transcripts from certain tissues at specific developmental stages or under certain physiological conditions. In order to analyze the transcriptomes of the left and right ovaries of the chick embryo at days 6 and 10, four sequencing libraries were prepared and sequenced using the Illumina paired-end technique. In total, there was 31,066,414 raw reads from 6R, 31,900,200 raw reads from 6L, 31,400,070 raw reads from 10R, and 35,504,746 raw reads from 10L. After the removal of the adapter, ambiguous, and low quality sequences, the raw reads were cleaned to produce 35,410,030 reads with a GC percentage of 51.39% for 6R, 31,293,780 reads with a GC percentage of 51.05% for 6L, 30,759,406 reads with a GC percentage of 49.90% for 10R, and 34,331,076 reads with a GC percentage of 50.04% for 10L. The Q20 contents were 98.70, 98.71, 98.60, and 98.77% for 6R, 6L, 10R, and 10L, respectively (Table 1). These reads were then used for the *de novo* assembly, and were high enough for further analyses of throughput and sequencing quality. The distributions of mapped or unmapped reads are shown in Table 2, following comparison with the unmapped gene from the ribosome reads and reference genome alignment TAB.

### *Analysis of chick embryo ovary gene annotation*

Using the Blastx program, sequences were first blasted against the smaller but well-annotated Swiss-Prot protein database, and then reads with no significant hits were blasted against the NR database. Gene names and descriptions were assigned to assembled sequences with the best blast matches (E, 0.001) to subjects in the database. Sequence similarity was searched against the NCBI NR database, which provides an estimated number of different genes expressed in the libraries, and 14,715 annotated sequences were detected after clustering the long sequences (94.88% of all unigenes), showing significant similarities to known proteins. The sequence homology of the left and right ovaries was further analyzed against the Nr database at days 6 and 10. Statistics for gene numbers in each group are shown in Table 3.

### *Differential transcribed genes*

To detect prolificacy-related gene changes, we determined the expression levels of all genes between 6R-VS-6L and 10R-VS-10L

**Table 3.** Gene number statistics for the 6R, 6L, 10R, and 10L groups

| | 6R | 6L | 10R | 10L |
|---|---|---|---|---|
| Known gene | 13,999 | 14,103 | 14,192 | 14,151 |
| New gene num | 1621 | 1652 | 1638 | 1638 |
| All gene num | 15,620 | 15,755 | 15,830 | 15,789 |

6R: Right ovary of the chick embryo at day 6; 6L: left ovary of the chick embryo at day 6; 10R: right ovary of the chick embryo at day 10; 10L: left ovary of the chick embryo at day 10.

in our RNA-Seq data based on gene expression profiles using FDR $\leq 0.001$ and the absolute value of log2 ratio $\geq 1$ as the threshold. The results showed that there were a large number of differentially expressed genes between the left and right ovary on days 6 and 10. On day 6, of the 539 unique differentially expressed genes between 6R and 6L, 251 were down-regulated and 288 were up-regulated. On day 10, 1046 DEGs were identified, with 799 being upregulated and 247 being down-regulated, respectively (Fig. 1). A volcano plot of differential gene expression shows all differentially expressed genes. Genes that were up regulated and down regulated between 6R-VS-6L and 10R-VS-10L are shown in Fig. 2 and Fig. 3.

### *Functional annotation*

To better understand the functions of differentially expressed genes. In addition to the static analysis of abundantly differentially expressed genes, over-represented biological processes at different stages of spermatogenesis can also be investigated by applying ontology analyses to clustered genes. Gene name and GO annotation provided an overview of each assigned sequence and the number of genes related to a specific process. The assembled sequences were categorized within three domains: biological processes, molecular functions, and cellular components. As shown, differentially expressed genes were detected in the left and right ovaries between days 6 and 10. To investigate the functions of the genes differentially expressed between 6R-VS-6L and 10R-VS-10L, the differentially expressed genes were mapped to terms in the GO database and compared with the transcriptome background. For 6R-VS-6L, the top 30 most highly enriched GO terms are presented in Fig. 4, which shows that a high percentage of differentially expressed genes were mapped. Under the biological process category, ‘cellular process’ was prominently represented. Within these cellular components, ‘cell’ and ‘cell part’ were the most highly represented categories. For the molecular

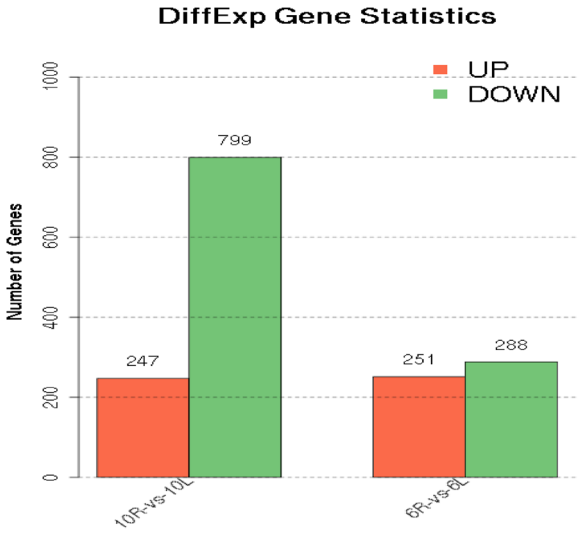


**Fig. 1.** Differentially expressed genes of 6R-VS-6L and 10R-VS-10L. 6R: Right ovary of the chick embryo at day 6; 6L: left ovary of the chick embryo at day 6; 10R: right ovary of the chick embryo at day 10; 10L: left ovary of the chick embryo at day 10.

function category, the largest proportion of genes was clustered into the 'binding' category. Among the down-regulated GO terms, the cellular components, 'cellular process' and 'single-organism process' were the most significant GO terms. Interestingly, for 10R-VS-10L, differences in up-regulated genes were not obvious, and the down-regulation of genes was significant compared to 6R-VS-6L. These results are shown in Fig. 5.

*KEGG pathways*

To explore the pathways in which these annotated genes were contained, KEGG analysis with E values ≤ $1e^{-10}$ was used to classify functional annotations of the differentially expressed genes to further understand their biological functions. KEGG is a database resource used to determine the high-level functions and utilities of biological systems from molecular-level information, especially large-scale molecular datasets generated by genome sequencing and other high-throughput experimental technologies [26]. Among the genes differentially expressed between 6R-VS-6L and 10R-VS-10L, 129 differences in the expression of unigenes were significantly matched to the database and were assigned to 96 KEGG pathways in the 6R-VS-6L group. The 265 different unigenes in the 10R-VS-10L group were assigned to 116 KEGG pathways, which were based on five KEGG modules: metabolism, environmental information processing, genetic information processing, cellular processes, and organismal systems.

In the 6R-VS-6L and 10R-VS-10L samples, the 20 most dominant enriched pathways featuring the highest RPKM values are shown in Fig. 6 and Fig. 7, respectively. Furthermore, the possible functions of unigenes were assessed according to similarity matches with the GO and KEGG databases. The result of these database searches helped us to understand the biological features of the Chinese surf clam.

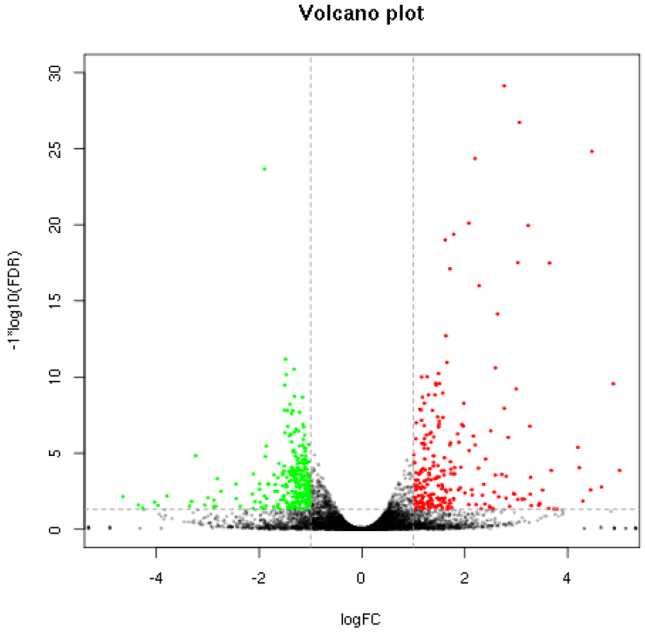


**Fig. 2.** Volcano plot analysis of differential expression in 6R-VS-6L. 6R: Right ovary of the chick embryo at day 6; 6L: left ovary of the chick embryo at day 6; 10R: right ovary of the chick embryo at day 10; 10L: left ovary of the chick embryo at day 10.

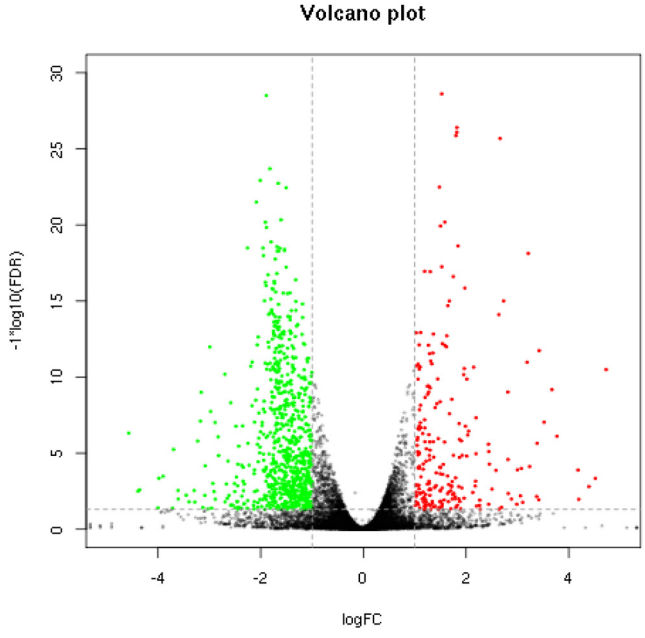


**Fig. 3.** Volcano plot analysis of differential expression in 10R-VS-10L. 6R: Right ovary of the chick embryo at day 6; 6L: left ovary of the chick embryo at day 6; 10R: right ovary of the chick embryo at day 10; 10L: left ovary of the chick embryo at day 10.

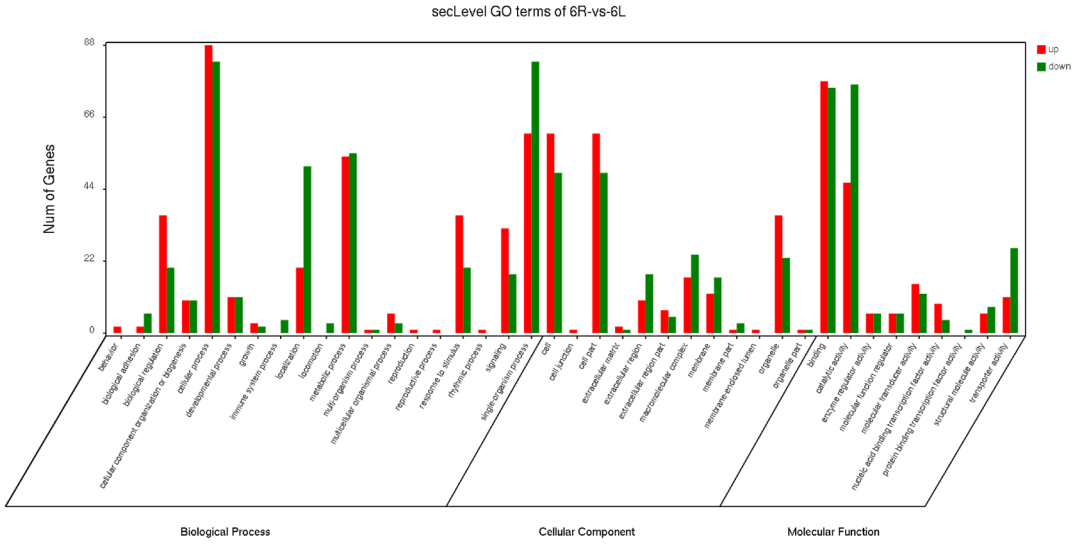


**Fig. 4.** GO analysis of differentially expressed genes from 6R-VS-6L. 6R: Right ovary of the chick embryo at day 6; 6L: left ovary of the chick embryo at day 6; 10R: right ovary of the chick embryo at day 10; 10L: left ovary of the chick embryo at day 10.

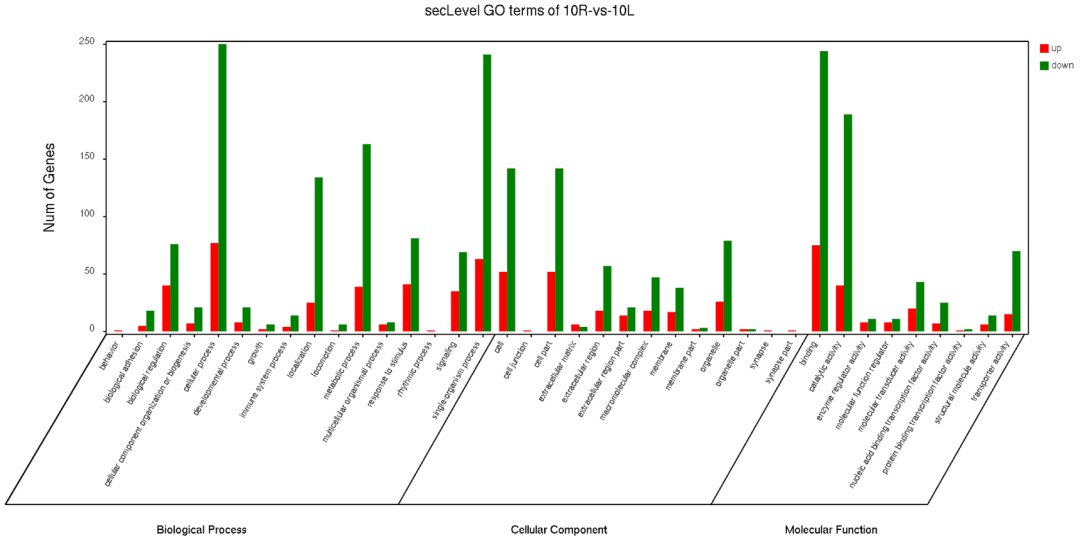


**Fig. 5.** GO analysis of differentially expressed genes from 10R-VS-10L. 6R: Right ovary of the chick embryo at day 6; 6L: left ovary of the chick embryo at day 6; 10R: right ovary of the chick embryo at day 10; 10L: left ovary of the chick embryo at day 10.

### *Identification of functional genes related to right ovary degeneration*

Attempts to understand the mechanisms of right ovary degradation represent an active research area. In an attempt to identify key genes involved in the degradation of the right ovary, focus was placed on those DEGs likely to be associated with apoptosis. The mapping of reads for the right and left ovary at different time points revealed differences in gene expression. Significantly, pathway-based analysis revealed that right ovary degradation was significantly ($P < 0.001$ and $P = 0.02$, respectively) related to apoptosis. In the 6R-VS-6L group (Fig. 8), our results revealed upregulation of the TNF-R1, NGF, and P13k genes in the left ovary, leading to IKK activation and the promotion of apoptosis. However, in the 10R-VS-10L group, compared with 10L, 10R showed that the initiation of apoptosis relies upon TrkA upregulation (Figs. 9 and 10), which promotes apoptosis. Other differentially expressed genes were less direct regulators of apoptosis.

### *RT-PCR*

Three genes from 6R-VS-6L known to be involved in the apoptotic pathway, and four genes from 10R-VS-10L known to be involved in the apoptotic pathway were collected, and their relative expression

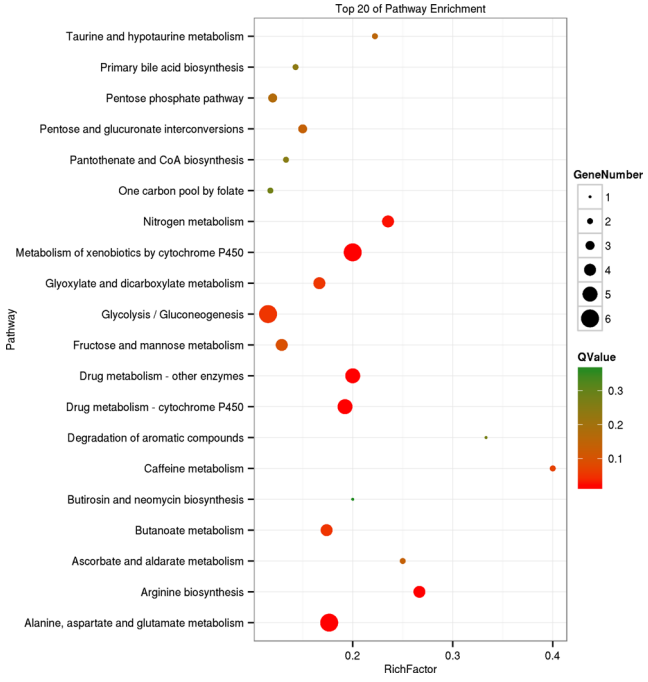


**Fig. 6.** The top 20 pathways enriched from GO analysis in 6R-VS-6L. 6R: Right ovary of the chick embryo at day 6; 6L: left ovary of the chick embryo at day 6; 10R: right ovary of the chick embryo at day 10; 10L: left ovary of the chick embryo at day 10.

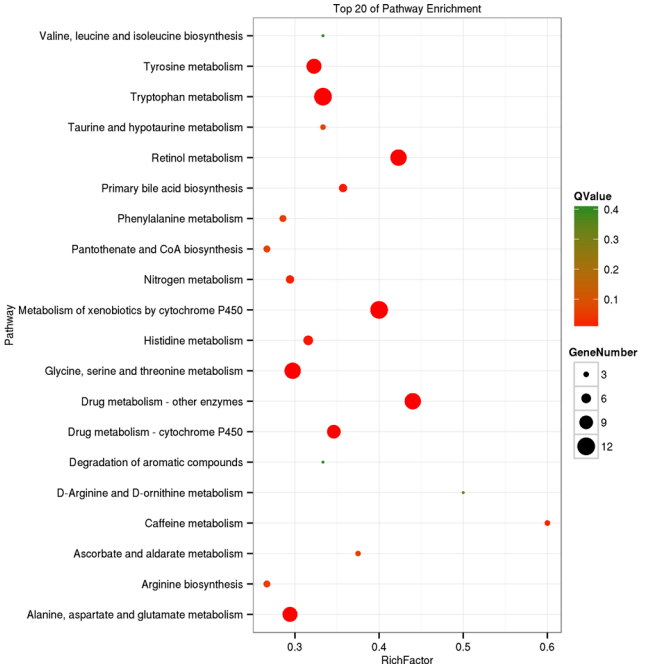


**Fig. 7.** The top 20 pathways enriched from GO analysis in 10R-VS-10L. 6R: Right ovary of the chick embryo at day 6; 6L: left ovary of the chick embryo at day 6; 10R: right ovary of the chick embryo at day 10; 10L: left ovary of the chick embryo at day 10.

was quantified by RT-PCR. As shown in Fig. 10, compared to the 6R sample, expression of the PI3K gene in the 6L sample was significantly up regulated. In addition, the TrkA gene from the 10R sample was clearly up regulated compared with that of the 10L sample.

## Discussion

Examination of the transcriptome can provide gene expression data, which can be used to detect expression signatures associated with phenotypes of interest, such as degeneration. Regulatory mechanisms involved in right ovary degeneration of the chick embryo have aroused the interest of researchers. However, few studies have been performed because of the limited amount of molecular data available. To understand transcriptional changes in gene expression, high-throughput RNA-seq technologies, including Roche/454 pyrosequencing and Illumina/Solexa sequencing, have led to a revolution in the fields of transcriptomics and genome characterization in recent years. Traditional methods can examine one gene at a time and provide data on the expression richness of many genes of interest. However, the information obtained is slow to accumulate, making it difficult to obtain a comprehensive view of the global changes in gene expression. Therefore, the Illumina HiSeq 2000 platform, which has the biggest output and lowest reagent costs, has been widely used for deep sequencing of model and non-model organisms [27–30].

In our study, differences in the gene expression profiles of 6R-VS-6L and 10R-VS-10L of the chick embryo ovary were investigated. To the best of our knowledge, this is the first report of a remarkable ovary development. We generated 31,066,414 sequence reads in the 6R sample, 31,900,200 sequences reads in the 6L samples, 31,400,070 sequences reads in the 10R samples, and 35,504,746 sequences reads in the 10L samples corresponding to sequencing data. Among these data, approximately 73.33% of the sequences could be mapped onto the reference genome sequence of the chick embryo ovary. This large dataset resulted in a relatively high sequencing depth.

Development of the chick embryo ovary is a complex physiological process, which is regulated by many genes and signaling pathways. Based on the RNA-Seq results, 22 significantly different genes were identified between 6R-VS-6L and 10R-VS-10L. Those genes that were up- and down-regulated in the ovary have previously been shown to be essential for ovarian development and degeneration. The top 20 most differentially expressed ovarian genes with the highest transcribed levels were identified, and those genes were found to be closely associated with neuroactive ligand-receptor interaction, carbon metabolism, phagosome, and calcium signaling. Overall, therefore, these genes may promote the degeneration of the right ovary. However, the function and mechanism of the different pathways identified in this study are unclear and can be regarded as an important pool of candidate genes for future analyses.

Apoptotic cells have been previously detected in the ovaries of embryonic and post-hatched Japanese quail [31], as well as in the ovaries of hens during sexual maturation [32] and in laying hens [33]. This may suggest that apoptosis is involved in the degeneration of the right ovary. Proliferating cells have been recently found in the cortical layer of the left female gonad of 5–6.5-day-old chicken

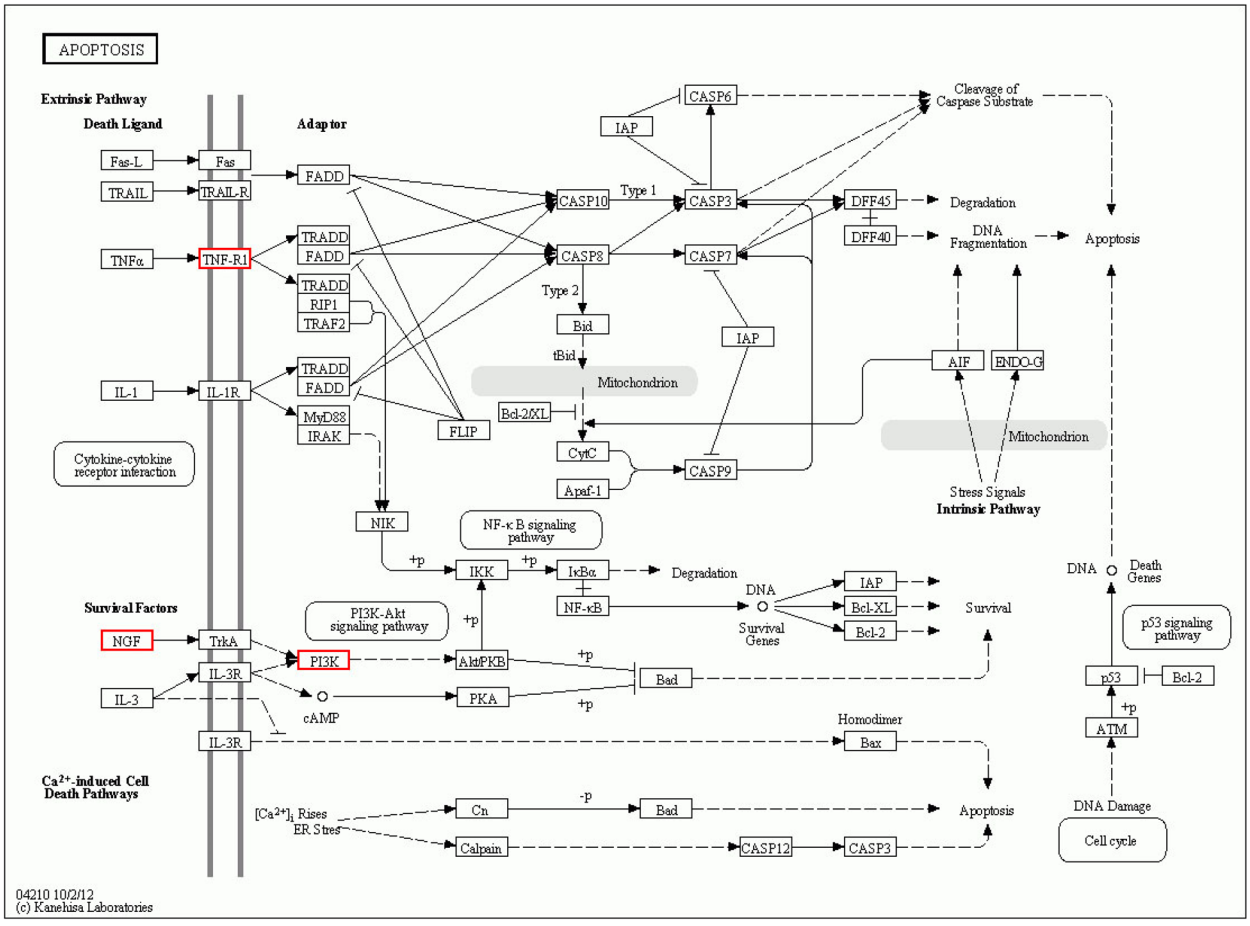


**Fig. 8.** The apoptotic pathway of 6R-VS-6L. 6R: Right ovary of the chick embryo at day 6; 6L: left ovary of the chick embryo at day 6; 10R: right ovary of the chick embryo at day 10; 10L: left ovary of the chick embryo at day 10. Red box: up regulated; Green box: down regulated.

embryos. However, cellular proliferation in differentiated chicken gonads during the second half of embryogenesis was not analyzed in that study. Therefore, a high or low (or absent) apoptotic index is the most interesting finding of the current study. Apoptosis is mainly associated with three main metabolic pathways, involving death ligands, survival factors, and $Ca^{2+}$-induced cell death.

Generally, apoptosis can be triggered *via* extrinsic and/or intrinsic signaling pathways, and the initiation of apoptosis is strictly controlled by caspases, mitochondria, and Bcl-2 family proteins. Caspases are families of cysteine-aspartic proteases or cysteine-dependent aspartate-directed proteases, which play essential roles in apoptosis. Caspases are classified into two families based on their function: three executioner caspases (caspase-3, caspase-6, and caspase-7) and four initiator caspases (caspase-2, caspase-8, caspase-9, and caspase-10). Bcl-2 family proteins are known to modulate apoptosis through the regulation of the mitochondrial apoptosis pathway. Bad, Bax, Bak, Bik, and HRK are promoters of apoptosis, while Bcl-2 functions as a major inhibitor of cell death, and therefore protects against apoptosis [34–36]. Mitochondria are important organelles for the generation of cellular energy, and are required for normal physiological functions. Mitochondria have also been shown to play a central role in the apoptotic process [37]. In the mitochondrial apoptotic pathway, BAX and BAK activate pro-apoptotic effectors, which disrupt the mitochondrial outer membrane resulting in the release of cytochrome c. In addition, deregulation of the mitochondrial apoptotic pathway, through BCL2, plays an important role in the progression of cellular degeneration.

In the present study, we used pathway act network analysis to investigate DEGs, with pathway annotation under different groups through RNA-Seq analysis. The results showed that among the survival factors, only the P13-Akt signaling pathway differed significantly between 6R and 6L. However, in the 10R-VS-10L group, FAS and IL-1 of the death ligand and P13-Akt signaling pathways were identified with notable differences among the survival factors. Activated FAS and IL-1 pathways in the 10L groups are implicated in processes such as apoptosis and DNA damage. The up-regulated FAS can usually activate caspase-8 and caspase-10, which further lead to downstream activation of effector caspases, such as caspase-3 and caspase-7, committing the cells to apoptosis and degeneration. In addition, the up-regulated IL-1 induced the expression of cytochrome c, which is a critical activator of procaspase-9 *via* the formation of the apoptosome together with Apaf-1 and Apaf-1. Apaf-1 and Apaf-1

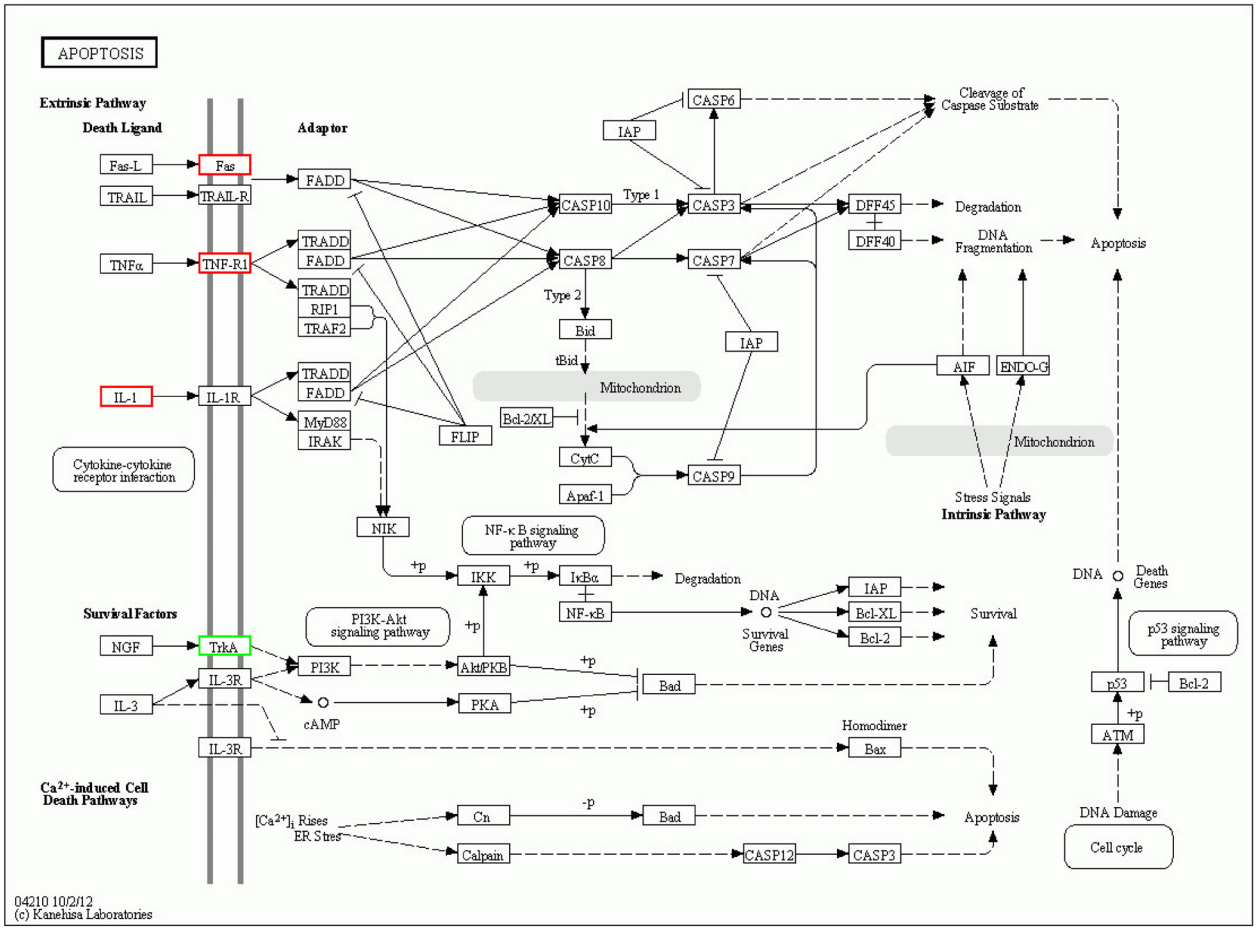


**Fig. 9.** The apoptotic pathway of 10R-VS-10L. 6R: Right ovary of the chick embryo at day 6; 6L: left ovary of the chick embryo at day 6; 10R: right ovary of the chick embryo at day 10; 10L: left ovary of the chick embryo at day 10. Red box: up regulated; Green box: down regulated.

induce downstream factors of the casp9 family; these activate "effector caspases" such as caspase-3, which cleave the death substrates and commit the cells to apoptosis. In addition, the findings of our study suggest that the IL-1 pathway can induce *IKK* gene expression and could be promising targets for improving the cell degradation. The down-regulated TrkA can inhibit the *BCL* pathway, which commits the cell to apoptosis.

To our knowledge, this is the first report on transcriptome sequencing and assembly in chicken embryos between 6R-VS-6L and 10R-VS-10L. This approach is crucially important, since it will help us to understand the molecular mechanisms involved in cellular differentiation in different development stages. The discovery of novel pathways involved in right ovary degeneration confirms the advantage of this approach. In addition, the results from this study will facilitate the further analysis of molecular mechanisms involved in the regulation of right ovary degeneration in the chick embryo.

## Acknowledgments

This study was supported by the Fund for Independent Innovation of Agricultural Sciences in Jiangsu Province [CX(14)2068], and Natural Science Foundation of Jiangsu Province (BK20140753).

## References

1. **Duan J, Shao F, Shao Y, Li J, Ling Y, Teng K, Li H, Wu C.** Androgen inhibits abdominal fat accumulation and negatively regulates the PCK1 gene in male chickens. *PLoS ONE* 2013; **8**: e59636. [Medline] [CrossRef]
2. **Silva C, Wood JR, Salvador L, Zhang Z, Kostetskii I, Williams CJ, Strauss JF 3rd.** Expression profile of male germ cell-associated genes in mouse embryonic stem cell cultures treated with all-trans retinoic acid and testosterone. *Mol Reprod Dev* 2009; **76**: 11–21. [Medline] [CrossRef]
3. **Carlon N, Stahl A.** Origin of the somatic components in chick embryonic gonads. *Arch Anat Microsc Morphol Exp* 1985; **74**: 52–59. [Medline]
4. **Ayers KL, Lambeth LS, Davidson NM, Sinclair AH, Oshlack A, Smith CA.** Identification of candidate gonadal sex differentiation genes in the chicken embryo using RNA-seq. *BMC Genomics* 2015; **16**: 704. [Medline] [CrossRef]
5. **Garber M, Grabherr MG, Guttman M, Trapnell C.** Computational methods for transcriptome annotation and quantification using RNA-seq. *Nat Methods* 2011; **8**: 469–477. [Medline] [CrossRef]
6. **Gibbons JG, Janson EM, Hittinger CT, Johnston M, Abbot P, Rokas A.** Benchmarking next-generation transcriptome sequencing for functional and evolutionary genomics. *Mol Biol Evol* 2009; **26**: 2731–2744. [Medline] [CrossRef]
7. **MacLean D, Jones JDG, Studholme DJ.** Application of next-generation sequencing

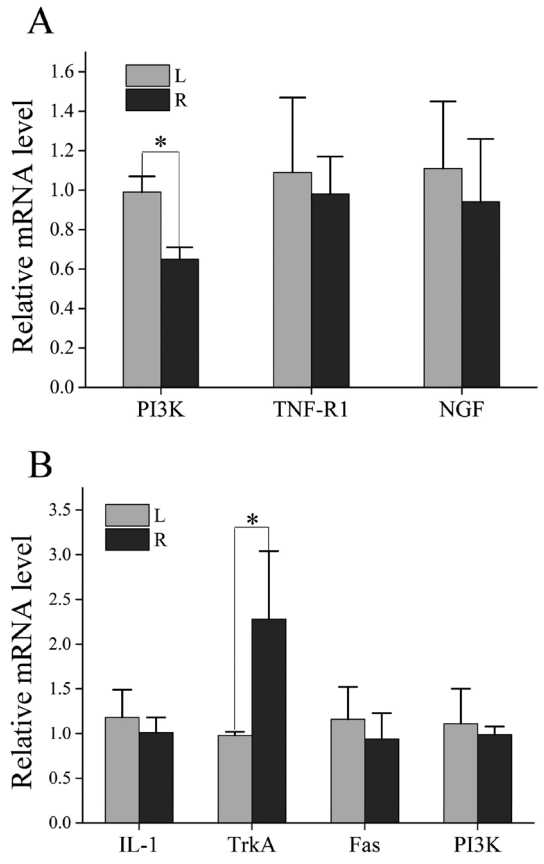


**Fig. 10.** Real-time PCR validation. A: 6R-VS-6L; B: 10R-VS-10L. L: the left sample; R: the right sample. 6R: Right ovary of the chick embryo at day 6; 6L: left ovary of the chick embryo at day 6; 10R: right ovary of the chick embryo at day 10; 10L: left ovary of the chick embryo at day 10. *P < 0.05.

technologies to microbial genetics. *Nat Rev Microbiol* 2009; **7**: 287–296. [Medline]

8. **Pop M, Salzberg SL.** Bioinformatics challenges of new sequencing technology. *Trends Genet* 2008; **24**: 142–149. [Medline] [CrossRef]
9. **Trombetti GA, Bonnal RJP, Rizzi E, De Bellis G, Milanesi L.** Data handling strategies for high throughput pyrosequencers. *BMC Bioinformatics* 2007; **8**(Suppl 1): S22. [Medline] [CrossRef]
10. **Li C, Wang Y, Huang X, Li J, Wang H, Li J.** De novo assembly and characterization of fruit transcriptome in Litchi chinensis Sonn and analysis of differentially regulated genes in fruit in response to shading. *BMC Genomics* 2013; **14**: 552. [Medline] [CrossRef]
11. **Feng C, Chen M, Xu CJ, Bai L, Yin XR, Li X, Allan AC, Ferguson IB, Chen KS.** Transcriptomic analysis of Chinese bayberry (Myrica rubra) fruit development and ripening using RNA-Seq. *BMC Genomics* 2012; **13**: 19. [Medline] [CrossRef]
12. **Cardoso-Silva CB, Costa EA, Mancini MC, Balsalobre TW, Canesin LE, Pinto LR, Carneiro MS, Garcia AA, de Souza AP, Vicentini R.** De novo assembly and transcriptome analysis of contrasting sugarcane varieties. *PLoS ONE* 2014; **9**: e88462. [Medline] [CrossRef]
13. **Chen H, Zha J, Liang X, Bu J, Wang M, Wang Z.** Sequencing and de novo assembly of the Asian clam (Corbicula fluminea) transcriptome using the Illumina GAIIx method. *PLoS ONE* 2013; **8**: e79516. [Medline] [CrossRef]
14. **Teodoro JG, Branton PE.** Regulation of apoptosis by viral gene products. *J Virol* 1997; **71**: 1739–1746. [Medline]
15. **Kerr JF, Wyllie AH, Currie AR.** Apoptosis: a basic biological phenomenon with wide-ranging implications in tissue kinetics. *Br J Cancer* 1972; **26**: 239–257. [Medline] [CrossRef]
16. **Youle RJ, Strasser A.** The BCL-2 protein family: opposing activities that mediate cell death. *Nat Rev Mol Cell Biol* 2008; **9**: 47–59. [Medline] [CrossRef]
17. **Iglesias-Guimarais V, Gil-Guiñon E, Sánchez-Osuna M, Casanelles E, García-Belinchón M, Comella JX, Yuste VJ.** Chromatin collapse during caspase-dependent apoptotic cell death requires DNA fragmentation factor, 40-kDa subunit-/caspase-activated deoxyribonuclease-mediated 3-OH single-strand DNA breaks *J Biol Chem* 2013; **288**: 9200–9215. [Medline] [CrossRef]
18. **Taylor RC, Cullen SP, Martin SJ.** Apoptosis: controlled demolition at the cellular level. *Nat Rev Mol Cell Biol* 2008; **9**: 231–241. [Medline] [CrossRef]
19. **Marchenko ND, Zaika A, Moll UM.** Death signal-induced localization of p53 protein to mitochondria. A potential role in apoptotic signaling. *J Biol Chem* 2000; **275**: 16202–16212. [Medline] [CrossRef]
20. **Sansome C, Zaika A, Marchenko ND, Moll UM.** Hypoxia death stimulus induces translocation of p53 protein to mitochondria. Detection by immunofluorescence on whole cells. *FEBS Lett* 2001; **488**: 110–115. [Medline] [CrossRef]
21. **Ye J, Fang L, Zheng H, Zhang Y, Chen J, Zhang Z, Wang J, Li S, Li R, Bolund L, Wang J.** WEGO: a web tool for plotting GO annotations. *Nucleic Acids Res* 2006; **34**: W293-7. [Medline] [CrossRef]
22. **Akazawa Y, Isomoto H, Matsushima K, Kanda T, Minami H, Yamaghchi N, Taura N, Shiozawa K, Ohnita K, Takeshima F, Nakano M, Moss J, Hirayama T, Nakao K.** Endoplasmic reticulum stress contributes to Helicobacter pylori VacA-induced apoptosis. *PLoS ONE* 2013; **8**: e82322. [Medline] [CrossRef]
23. **Mortazavi A, Williams BA, McCue K, Schaeffer L, Wold B.** Mapping and quantifying mammalian transcriptomes by RNA-Seq. *Nat Methods* 2008; **5**: 621–628. [Medline] [CrossRef]
24. **Quinlan AR, Hall IM.** BEDTools: a flexible suite of utilities for comparing genomic features. *Bioinformatics* 2010; **26**: 841–842. [Medline] [CrossRef]
25. **Wang L, Feng Z, Wang X, Wang X, Zhang X.** DEGseq: an R package for identifying differentially expressed genes from RNA-seq data. *Bioinformatics* 2010; **26**: 136–138. [Medline] [CrossRef]
26. **Kanehisa M, Araki M, Goto S, Hattori M, Hirakawa M, Itoh M, Katayama T, Kawashima S, Okuda S, Tokimatsu T, Yamanishi Y.** KEGG for linking genomes to life and the environment. *Nucleic Acids Res* 2008; **36**: D480–D484. [Medline] [CrossRef]
27. **De Donato M, Peters SO, Mitchell SE, Hussain T, Imumorin IG.** Genotyping-by-sequencing (GBS): a novel, efficient and cost-effective genotyping method for cattle using next-generation sequencing. *PLoS ONE* 2013; **8**: e62137. [Medline] [CrossRef]
28. **Huang HH, Xu LL, Tong ZK, Lin EP, Liu QP, Cheng LJ, Zhu MY.** De novo characterization of the Chinese fir (Cunninghamia lanceolata) transcriptome and analysis of candidate genes involved in cellulose and lignin biosynthesis. *BMC Genomics* 2012; **13**: 648. [Medline] [CrossRef]
29. **Petrini I, Rajan A, Pham T, Voeller D, Davis S, Gao J, Wang Y, Giaccone G.** Whole genome and transcriptome sequencing of a B3 thymoma. *PLoS ONE* 2013; **8**: e60572. [Medline] [CrossRef]
30. **Xie C, Li B, Xu Y, Ji D, Chen C.** Characterization of the global transcriptome for Pyropia haitanensis (Bangiales, Rhodophyta) and development of cSSR markers. *BMC Genomics* 2013; **14**: 107. [Medline] [CrossRef]
31. **Zhai R, Feng Y, Wang H, Zhan X, Shen X, Wu W, Zhang Y, Chen D, Dai G, Yang Z, Cao L, Cheng S.** Transcriptome analysis of rice root heterosis by RNA-Seq. *BMC Genomics* 2013; **14**: 19. [Medline] [CrossRef]
32. **Yoshimura Y, Nishikori M.** Identification of apoptotic oocytes in the developing ovary of embryonic and post-hatched chicks in Japanese Quail (Coturnix japonica). *Jpn Poult Sci* 2004; **41**: 64–68. [CrossRef]
33. **Hrabia A. Janko's E.** Effect of short-term fasting on caspase and estrogen receptor gene expression in the chicken ovary. *Acta Biol Cracov Ser Zool* 2011; **53**: 25–30.
34. **Cory S, Huang DC, Adams JM.** The Bcl-2 family: roles in cell survival and oncogenesis. *Oncogene* 2003; **22**: 8590–8607. [Medline] [CrossRef]
35. **Story M, Kodym R.** Signal transduction during apoptosis; implications for cancer therapy. *Front Biosci* 1998; **3**: d365–d375. [Medline] [CrossRef]
36. **Dixon SC, Soriano BJ, Lush RM, Borner MM, Figg WD.** Apoptosis: its role in the development of malignancies and its potential as a novel therapeutic target. *Ann Pharmacother* 1997; **31**: 76–82. [Medline] [CrossRef]
37. **Cory S, Adams JM.** The Bcl2 family: regulators of the cellular life-or-death switch. *Nat Rev Cancer* 2002; **2**: 647–656. [Medline] [CrossRef]